



Spatial-temporal variations in riverine carbon strongly influenced by local hydrological events in an alpine headwater stream

Xin Wang^{1,2#}, Ting Liu^{1#}, Liang Wang¹, Zongguang Liu^{1,2}, Erxiong Zhu^{1,2}, Simin Wang^{1,2}, Yue Cai^{1,2}, Shanshan Zhu^{1,2}, Xiaojuan Feng^{1,2*}

5 ¹ State Key Laboratory of Vegetation and Environmental Change, Institute of Botany, Chinese Academy of Sciences, Beijing, 100093, China

² College of Resources and Environment, University of Chinese Academy of Sciences, Beijing, 100049, China

These authors contribute equally to this work.

Correspondence to: Xiaojuan Feng (xfeng@ibcas.ac.cn)

10 **Abstract.** Headwater streams drain > 70% of global land areas but are poorly monitored compared with large rivers. The small size and low water buffering capacity of headwater streams may result in a high sensitivity to local hydrological alterations and divergent carbon transport dynamics relative to large rivers. To assess these aspects, here we carry out a benchmark investigation on the riverine carbon dynamics in a typical alpine headwater stream (Shaliu River) on the Qinghai-Tibetan Plateau based on annual flux monitoring, in-depth seasonal sampling and hydrological event monitoring. We show
15 that riverine carbon in the Shaliu River was dominated by dissolved inorganic carbon, peaking in the summer due to high discharge brought by the monsoon. Combining seasonal sampling along the river and monitoring of soil-river carbon transfer during spring thaw, we also show that both dissolved and particulate forms of riverine carbon increased downstream in the pre-monsoon season due to increasing contribution of organic matter derived from thawed permafrost along the river. By comparison, riverine carbon fluctuated in the summer, likely associated with sporadic inputs of organic matter supplied by
20 local precipitation events during the monsoon season. Furthermore, using lignin phenol analysis for both riverine organic matter and soils in the basin, we show that the higher acid-to-aldehyde (Ad/Al) ratios of riverine lignin in the monsoon season reflect a larger contribution of topsoil likely via increased surface runoff compared with the pre-monsoon season when soil leachate lignin Ad/Al ratios were closer to those in the subsoil than topsoil solutions. Overall, these findings highlight the unique patterns and strong links of carbon dynamics in alpine headwater streams with local hydrological events.
25 Given the projected climate warming on the Qinghai-Tibetan Plateau, thawing of seasonal permafrost and alterations of precipitation regimes may significantly influence the alpine headwater carbon dynamics, with cascading effects on the biogeochemical cycles of the watersheds. The alpine headwater streams may also be utilized as sentinels for climate-induced changes in the hydrological pathways and/or biogeochemistry of the small basin.

1. Introduction

30 Headwater streams, including first- and second-order streams (Meyer and Wallace, 2001), comprise nearly 90% of the total length of global river networks (Downing et al., 2012) and drain > 70% of global land areas (Gomi et al., 2002). They are



hence important sources of water, sediment, organic matter and nutrients for downstream regions (Gomi et al., 2002) and critical for maintaining ecological functions of the entire fluvial system including biogeochemical cycling (Biggs et al., 2017). However, headwater streams remain under-investigated in terms of biogeochemical processes and carbon transport dynamics compared with large rivers so far, constraining an accurate understanding of the “boundless carbon cycle” (Battin et al., 2009).

Headwater streams differ from large rivers in several aspects that may affect their carbon transport dynamics. First, headwater streams have narrower width and shallower depth than large rivers, and are closely connected with adjacent terrestrial ecosystems via water and solute exchange (Battin et al., 2009; Öquist et al., 2014). Second, headwater streams have smaller drainage areas and buffering capacity for water flow than large rivers (McMahon and Finlayson, 2003; Rivenbark and Jackson, 2004; Svec et al., 2005). In addition, water in headwater streams has a shorter residence time (Caillon and Schelker, 2020). The above characteristics collectively result in high sensitivity of headwater streams to local hydrological alterations or sporadic events such as precipitation (Benda et al., 2005; Hassan et al., 2005; Richardson et al., 2005). Thus, riverine carbon dynamics in headwater streams may show a fast and strong response to local environmental variations and are receiving increasing attention (Gomi et al., 2002; Jaffé et al., 2012; Mann et al., 2015; Biggs et al., 2017) to improve our understanding of riverine carbon cycling (Flury and Ulseth, 2019; French et al., 2020; Battin et al., 2009).

Studies on headwater carbon dynamics have largely examined tropical and temperate streams in association with rainstorm events (Pereira et al., 2014; Argerich et al., 2016; Johnson et al., 2006; Waterloo et al., 2006). By comparison, headwater streams residing in alpine regions that are heavily affected by freeze-thaw and snow melting events are less well studied (Mann et al., 2015; Bröder et al., 2020; Chiasson-Poirier et al., 2020). The Qinghai-Tibetan Plateau, known as the “Asian Water Tower”, harbors numerous headwater streams for seven major Asian rivers (Immerzeel et al., 2010; Qiu, 2008). This region is covered by large areas of glaciers and seasonal permafrost and is significantly affected by the summer monsoon (Zou et al., 2017), likely resulting in unique seasonal patterns regarding riverine carbon dynamics compared to headwater streams in other regions such as the Arctic or tropical rivers (Zhang et al., 2013). Furthermore, as one of the most climate-sensitive regions, warming-induced alterations of permafrost dynamics and precipitation patterns may change the hydrogeological characteristics of headwater streams (Chang et al., 2018) and thus affect riverine carbon dynamics. However, the variations of riverine carbon and its response to thawing and precipitation events in headwater streams on the Qinghai-Tibetan Plateau are poorly resolved.

Here we investigate riverine carbon dynamics in a typical headwater stream (Shaliu River) feeding into the Qinghai Lake on the Qinghai-Tibetan Plateau at three different levels. First, we provide a year-long biweekly monitoring record on the water discharge and concentrations of dissolved organic carbon (DOC) and dissolved inorganic carbon (DIC) to assess annual fluvial carbon fluxes on a monthly basis. Second, we use bulk and biomarker (lignin phenols) analyses to examine riverine carbon composition and its variations along the Shaliu River by dense sampling in both pre-monsoon (spring thawing) and monsoon seasons. Third, to further identify the influence of hydrological events on the spatial-temporal variations of riverine carbon, we examine carbon transport from the adjacent soils to the stream during a 79-day thawing

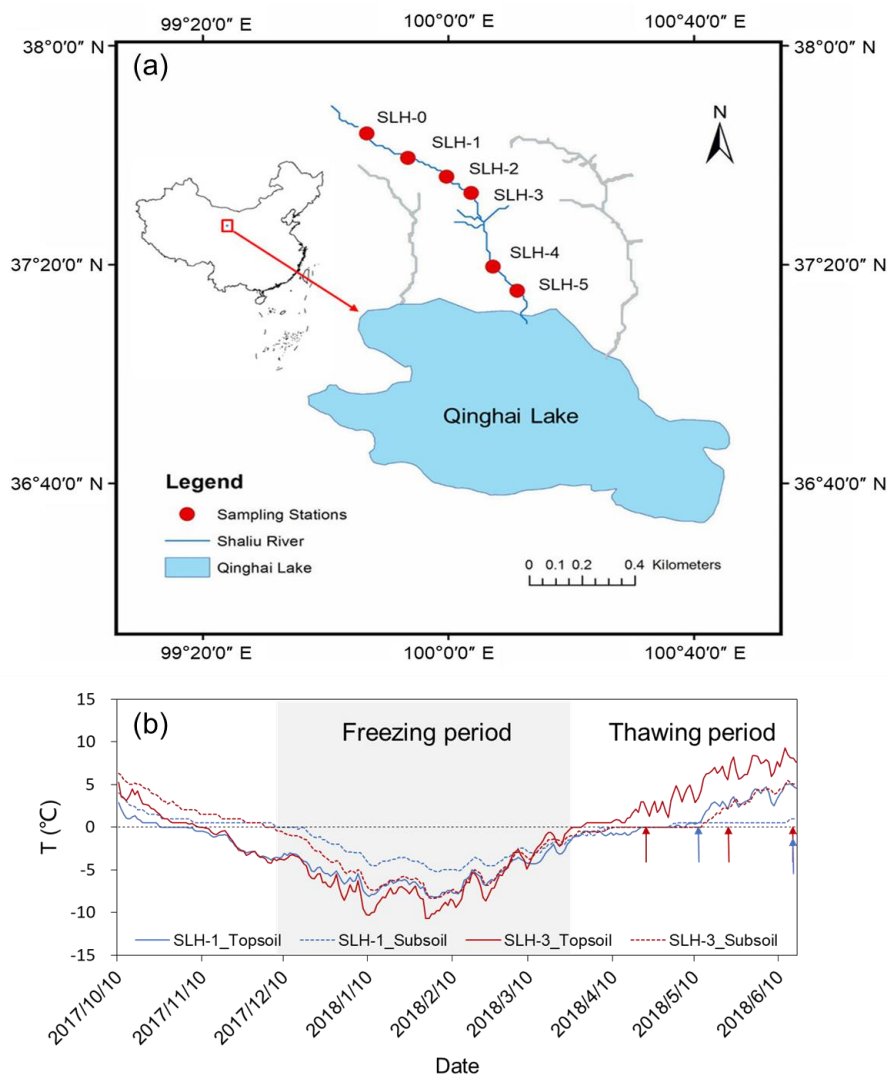


period and a short-term monsoon precipitation event. Collectively, these investigations provide a benchmark illustration of riverine carbon dynamics in a typical headwater stream on the Qinghai-Tibetan Plateau.

2. Materials and Methods

2.1 Study area

70 The Shaliu River, with a length of 110 km and a basin area of 1442 km² (Zhang et al., 2013), is the second largest stream
flowing into the Qinghai Lake on the northeastern edge of Qinghai-Tibetan Plateau at an altitude of 3200–3800 m above sea
level (Figure 1a). It flows through a semiarid alpine region widely covered by seasonal permafrost (Zhang and Li, 2018;
Wang et al., 2018) and is relatively well protected from human activities (Zhang et al., 2013; Cheng et al., 2018). The Shaliu
River basin is covered by grassland (~71%) dominated by *Potentilla anserina Rosaceae*, *Elymus nutans Griseb*, and *Deyeuxia*
75 *arundinacea* (Liu et al., 2018), bare land (16%) and wetland (10%; Cheng et al., 2018). Soils in the basin are mainly Gelic
Cambisol (IUSS working group WRB, 2015). The mean annual temperature is -0.5°C within the basin (Li et al., 2013) and
mean annual precipitation is 370 mm, ~90% of which occurs in the monsoon season (June to September; Zhang et al., 2013;
Wu et al., 2019). The active layer of seasonal permafrost in the watershed starts to thaw in late April to early May (i.e., pre-
monsoon season) and refreezes in late October. The stream is partly or fully frozen from November to March.



80

Figure 1. Sampling sites along the Shaliu River (a) and soil temperature (T) at the depth of 10 cm (referred as topsoil) and 40 cm (subsoil) at SLH-1 and SLH-3 stations (b). The map in panel (a) was processed with ArcGIS 10.0. The blue and red arrows in panel (b) indicated the collection time of soil solution at SLH-1 and SLH-3 stations during thawing event, respectively.

85 2.2 Sample collection

For annual flux assessment, the daily discharge of the Shaliu River was obtained from Gangcha hydrological station (SLH-4) where river water was collected biweekly from the middle of stream using pre-washed high-density polyethylene containers from May 2015 to April 2016. An aliquot of the water was immediately filtered through 0.45- μm acetate syringe filters and preserved with 0.02% saturated mercury chloride (HgCl_2) in vials without headspace in the dark for DIC analysis. The



90 remaining water was filtered through pre-combusted (550°C, 4 h) and pre-weighted 0.7- μm GF/F filters, preserved with a few drops of saturated HgCl_2 , and kept frozen in acid-washed glass vials until DOC analysis.

For seasonal water sampling, river water was collected using the same method as above at five evenly-distributed stations along the Shaliu River in May (pre-monsoon season) and August (monsoon season), 2015 (Figure 1a; SLH-5 was only sampled in the pre-monsoon season). Water temperature, pH, dissolved oxygen (DO) and conductivity were measured in situ
95 using a multi-parameter device (ProfiLine Multi 3320, WTW, Germany). Waters were filtered and preserved as above for DIC and DOC analyses. Moreover, filtered waters (0.7 μm) were kept frozen before measuring nitrogen (N) species and cations. The filters were freeze-dried for total suspended solids (TSS), particulate organic carbon (POC), particulate inorganic carbon (PIC), particulate N and particulate lignin phenol measurements. The remaining filtrates were acidified to pH 2 and extracted by solid phase extraction (SPE) for dissolved lignin phenol measurements.

100 To assess the influence of local hydrological events on riverine carbon, we further monitored spring thawing and a monsoonal precipitation. Specifically, soil temperature was monitored at 10 and 40 cm beneath the surface at SLH-1 and SLH-3 stations (~150 m away from the river bank) at 2-h intervals from October 2017 to June 2018 using iButton Temperature Loggers (DS1922L, Wdsen, China). Spring thawing occurred in late April when soil temperature was $> 0^\circ\text{C}$ (Figure 1b). Soil solutions were collected two or three times from top- (0–10 cm) and subsoil (30–40 cm) using pre-arranged
105 ceramic head (0.2- μm) in April-June 2018. Soil leachates were also directly collected by putting acid-washed carboys under soil layers in exposed soil profiles in June 2018 (Wang et al., 2018). Soil solutions and leachates were filtered (0.22- μm) immediately upon collection and preserved as previously described for DOC and dissolved lignin phenol analyses. For the monsoonal precipitation, river water was sampled at 15-min intervals (four times) at SLH-4 station during a precipitation event (lasting for 1 hour) in August 2015, and filtered for the measurements of DOC, DIC, POC, PIC and TSS.

110 To investigate connections between riverine and soil organic matter within the basin, topsoil (0–10 cm) and subsoil (40–60 cm) samples were collected from five locations 150–500 m away from the corresponding river sampling station in August 2015. At each location, three soil cores were collected from each of three random quadrats (1 \times 1 m; intervals > 500 m) using a stainless steel gravity corer (diameter of 5 cm). Soils from the same depth and same quadrat were homogenized and shipped back to laboratory. Freeze-dried soils were passed through a 2-mm sieve for soil organic carbon (SOC), soil N and
115 soil lignin phenol measurements after removal of visible roots.

2.3 Bulk chemical analysis

The contents of riverine POC, particulate N, SOC and soil N were determined by elemental analyzer (Vario EL III, Germany) after fumigation with concentrated hydrochloric acid (HCl; Dai et al., 2019). POC concentration (mg L^{-1}) was calculated based on POC content (%OC) and TSS concentration. PIC was calculated by subtracting POC from total particulate carbon
120 quantified by elemental analyzer without fumigation.

The DOC, dissolved N and DIC concentrations were measured using a Multi N/C 3100 Analyzer (Analytik Jena, Germany). Inorganic N including ammonium ($\text{NH}_4^+\text{-N}$), nitrate ($\text{NO}_3^-\text{-N}$) and nitrite ($\text{NO}_2^-\text{-N}$) were determined



125 colorimetrically on an Autoanalyser-3 (Bran & Luebbe, Germany). Dissolved organic N (DON) was calculated by subtracting all inorganic N from dissolved N. Major cations including calcium (Ca) and magnesium (Mg) were measured on an inductively coupled plasma mass spectrometer (ICP-MS, 7700X, Agilent, USA) after acidifying to pH < 2.

2.4 Lignin phenol analysis

130 Lignin phenols were analyzed using the alkaline copper oxide (CuO) oxidation method to trace terrestrially derived OM (Hedges and Ertel, 1982). Filtered river water were acidified to pH 2, amended with pure methanol to a final concentration of 0.5% (v/v) (Spencer et al., 2010a) and passed through Mega Bond Elut C₁₈ SPE cartridges (5 g; Agilent, USA) by a peristaltic pump at a flow rate of 10 mL min⁻¹ to concentrate dissolved organic matter (DOM; Louchouart et al., 2010). All cartridges were dried and kept in a freezer in the dark until DOM was eluted with methanol and dried under nitrogen gas (N₂). Dried samples were mixed with 0.5 g CuO, 50 mg ammonium iron (II) sulfate hexahydrate [Fe(NH₄)₂(SO₄)₂•6H₂O] and 15 mg glucose (to avoid excessive oxidation), and soil solutions and leachates were mixed with the same reagents as well. All samples were mixed with 20 ml of 2 M N₂-purged sodium hydroxide (NaOH) solution in teflon-lined bombs at 135 170°C for 2.5 h. The lignin oxidation products (LOPs) were spiked with a recovery standard (ethyl vanillin), acidified to pH < 2 with 12-M HCl, and kept in the dark for 2 h. Oxidation products were extracted with ethyl acetate three times, spiked with an internal standard (trans-cinnamic acid), and concentrated under N₂ for further analysis. Lignin phenols, after converting to trimethylsilyl derivatives by reacting with N,O-bis-(trimethylsilyl)trifluoroacetamide (BSTFA) and pyridine, were quantified on a gas chromatograph-mass spectrometer (GC-MS; Thermo Fisher Scientific, USA) using a DB-5MS 140 column (30 m × 0.25 mm inner diameter; film thickness 0.25 μm) for separation (Dai et al., 2019). Quantification was achieved by comparing with recovery standards (ethyl vanillin) to account for compound loss during extraction procedures. In addition, TSS and soil samples were extracted using the same procedures as mentioned above without the addition of glucose.

145 Eight lignin-derived phenols, including vanillyl (V; vanillin, acetovanillone, vanillic acid), syringyl (S; syringaldehyde, acetosyringone, syringic acid), and cinnamyl (C; *p*-coumaric acid, ferulic acid) phenols, are used to represent the absolute (Σ₈; in the units of μg L⁻¹) and OC-normalized concentration (Λ₈; in the units of mg g⁻¹ OC) of lignin phenols. The acid-to-aldehyde (Ad/Al) ratios of V and S phenols are used to indicate lignin oxidation (Opsahl and Benner, 1995) but may be affected by leaching and sorption processes as well (Hernes et al., 2007).

2.5 Carbon flux estimate from LOADEST

150 The daily discharge was combined with measured DOC and DIC concentrations to model their fluxes using the USGS load estimator (LOADEST) program (Runkel et al., 2004; <https://water.usgs.gov/software/loadest/>) within the LoadRunner software package (URL: <https://environment.yale.edu/loadrunner/>). The best regression model from nine predefined regression models within LOADEST was select to fit the measured DOC (Equation 1) and DIC fluxes (Equation 2) for annual carbon flux estimate (Song et al., 2020; Tank et al., 2012; Bao et al., 2019; Raymond et al., 2007; Zolkos et al., 2018):



155 $\ln(\text{DOC flux}) = a_0 + a_1 \ln Q$ (1)

$$\ln(\text{DIC flux}) = a_0 + a_1 \ln Q + a_2 \ln Q^2 + a_3 \sin(2\pi \text{dtime}) + a_4 \cos(2\pi \text{dtime}) + a_5 \text{dtime} + a_6 \text{dtime}^2 \quad (2)$$

where flux is provided in kg day^{-1} , Q is river discharge ($\text{cubic feet sec}^{-1}$), $\ln Q$ equals $\ln(\text{streamflow})$ minus center of $\ln(\text{streamflow})$, dtime equals decimal time minus center of decimal time, other parameters (i.e., $a_0, a_1, a_2, a_3, a_4, a_5, a_6$) are shown in Table S1. LOADEST can provide daily, monthly and annually fluxes using adjusted maximum likelihood estimation (AMLE) approach (Song et al., 2020; Tank et al., 2012).

2.6 Statistical analyses

Normal distribution of data and homogeneity of variance were checked for all variables using Shapiro-Wilk and Levene tests, respectively. Differences in river water parameters between the pre-monsoon and monsoon seasons were tested using independent-sample t-test. Differences in the Ad/Al ratios between top- and subsoils were analyzed by paired t-test. Differences in river water pH were checked by Mann-Whitney U test due to non-normal distribution of data. Pearson correlation was used to assess relationships between DIC and cation concentrations and between riverine carbon concentration and the distance of sampling sites from SLH-0. Differences and correlations were considered to be significant at a level of $p < 0.05$. All statistical analyses were conducted using SPSS 25 (SPSS, Chicago, USA).

3. Results and Discussion

3.1 Riverine carbon fluxes in the Shaliu River

In contrast to Arctic rivers with a pronounced spring freshet from May to June, the maximum discharge in the Shaliu River appeared from July to August (Figure 2a) due to frequent precipitation events in the monsoon season. Accordingly, both DIC and DOC fluxes were highest in summer, accounting for 58-60% of the corresponding annual fluxes (Figure 2b). DIC was the dominant form of dissolved riverine carbon with a higher concentration in the monsoon ($30.7 \pm 2.3 \text{ mg L}^{-1}$) than pre-monsoon season ($25.3 \pm 1.9 \text{ mg L}^{-1}$; Figure S1a). DIC accounted for at least 87% of the total riverine carbon (including particulate carbon), which is generally higher than tropical (~40%; Huang et al., 2012) and Arctic rivers (52-70%; Striegl et al., 2007; Prokushkin et al., 2011; Guo et al., 2012) but similar to rivers sourced from the Qinghai-Tibetan Plateau including the upper Yangtze River, Yellow River and their tributaries (Cai et al., 2008; Gao et al., 2019; Song et al., 2019; Song et al., 2020). The large proportion of DIC in riverine carbon partly reflects the high chemical weathering rate on the Qinghai-Tibetan Plateau evidenced by the high riverine Ca^{2+} and Mg^{2+} concentrations (Zhang et al., 2013) and their positive correlations with DIC ($p < 0.05$; Figure S1b). Moreover, DIC concentration ($25.0\text{--}63.2 \text{ mg L}^{-1}$) showed a larger intraannual variability than DOC ($2.5\text{--}3.1 \text{ mg L}^{-1}$) at the Gangcha hydrological station (SLH-4) on the Shaliu River (Figure 2a), due to variable inputs of subsurface flow and groundwater containing high DIC in this permafrost-affected watershed (Walvoord and Striegl, 2007; Giesler et al., 2014). Overall, annual DIC flux was 8.0 Gg year^{-1} ($1 \text{ Gg} = 10^9 \text{ g}$), > 10 times larger than the DOC flux (0.6 Gg year^{-1}) in the Shaliu River, and constitutes 90% of the total dissolved carbon flux.

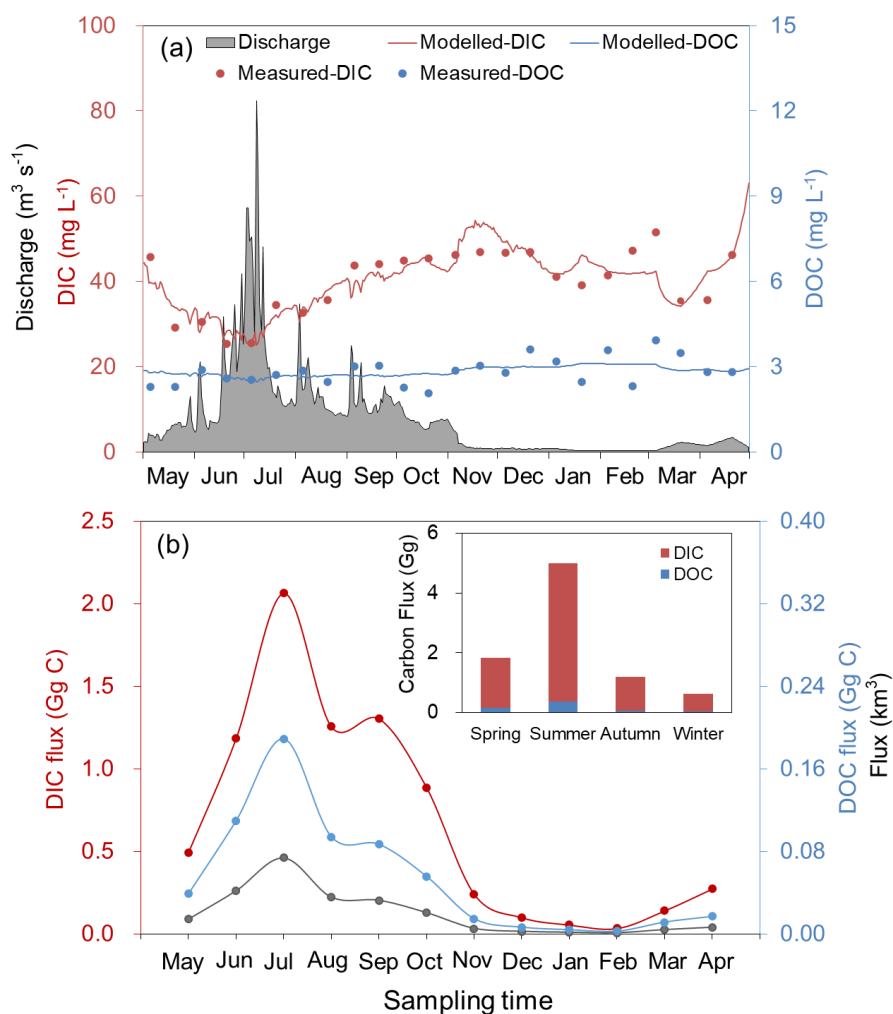


Figure 2. Discharge, dissolved inorganic carbon (DIC) and dissolved organic carbon (DOC) concentrations exported from Shaliu River at SLH-4 station (a), and monthly average DIC and DOC fluxes in Shaliu River during 2015 and 2016 (b). The model simulation data was obtained by load estimator (LOADEST). The inserted columns in panel (b) showed the seasonal variations of carbon fluxes classified as follows: spring (May to June), summer (July to September), autumn (October to November), and winter (December to the next April).

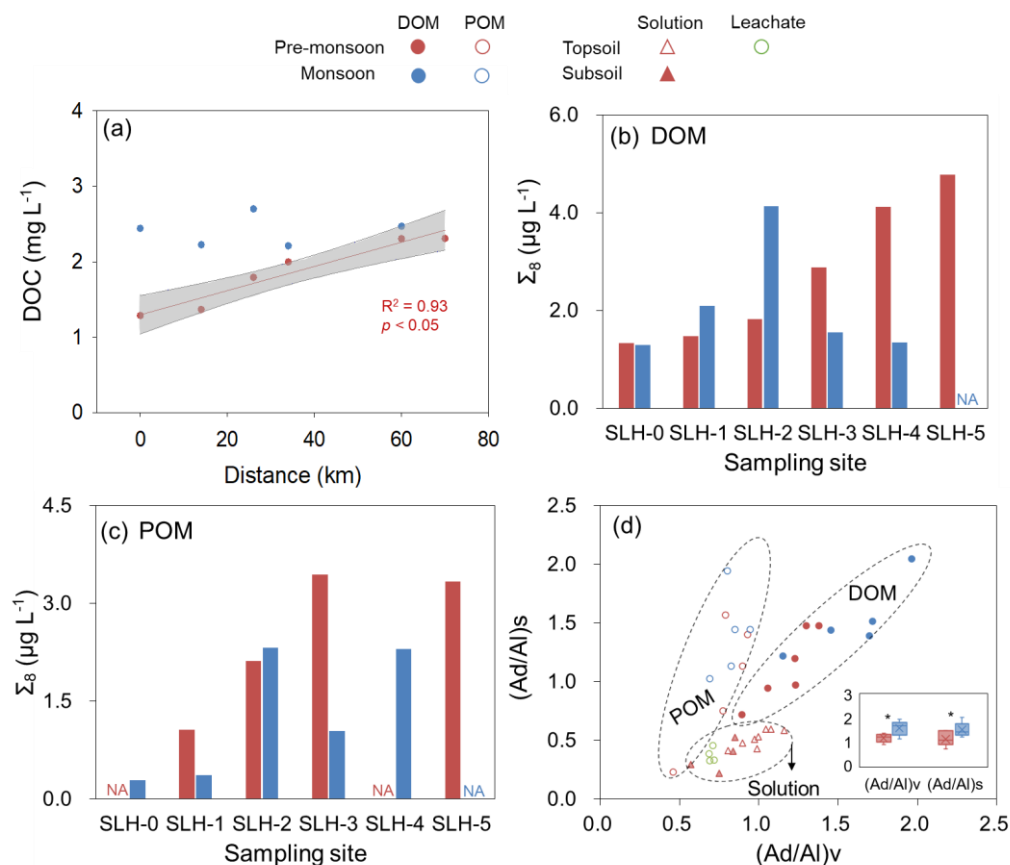
DOC was the second most abundant riverine carbon with a higher concentration in the monsoon ($2.4 \pm 0.1 \text{ mg L}^{-1}$) than pre-monsoon season ($1.8 \pm 0.2 \text{ mg L}^{-1}$; Figure S1a). Its concentration is lower in the Shaliu River than most Arctic rivers (Mann et al., 2016; Amon et al., 2012; Spencer et al., 2008), only accounting for 7% of total riverine carbon. However, its concentration is equivalent to the upper Yangtze, Yellow and Yarlung Zangbo Rivers (Qu et al., 2017; Ran et al., 2013). The low DOC concentration reflects the relatively low SOC density in the alpine grasslands of the Qinghai-Tibetan Plateau (9.05



kg C m⁻² in 0–100 cm depth; Yang et al., 2008) compared to most Arctic river basins containing organic matter-rich peatlands and deposits (32.2–69.6 kg C m⁻²; Tarnocai et al., 2009). The concentration of dissolved inorganic N ranged from 0.8 to 3.0 mg L⁻¹, followed by DON (0.3–0.5 mg L⁻¹; Table S2), resulting in DOC/DON ratios of 5–11 (8.2 ± 1.1; Table S2). The low DOC/DON ratios in the Shaliu River relative to the global riverine average (14; Harrison et al., 2005; Seitzinger et al., 2005) potentially indicate high biodegradability of riverine DOM (Wiegner et al., 2006), which may also contribute to the low DOC concentration in this river.

3.2 Spatial-temporal variation of riverine carbon in the Shaliu River

Both dissolved (i.e., DOC and DIC) and particulate carbon (i.e., POC and PIC) concentrations fluctuated along the Shaliu River in the monsoon season, while most of them increased significantly downstream in the pre-monsoon season ($p < 0.05$; Figure 3a) except for a marginally significant increasing trend for POC ($p = 0.07$; Figure S2). Similarly, the absolute concentration of dissolved and particulate lignin phenols (Σ_8) peaked at SLH-2 in the monsoon season, but they showed a downstream increasing trend in the pre-monsoon season (Figures 3b-c). The downstream increases of particulate carbon and lignin phenols were correlated with TSS concentrations in the pre-monsoon season ($p < 0.05$; $r = 0.93$). These trends stand in contrast to the downstream accumulation of riverine carbon in the high flow and increasing degradation in the low flow conditions observed in other rivers including Zambezi River (Lambert et al., 2016) and a tributary of Yukon River (Dornblaser and Striegl, 2015), suggesting unique seasonality in the spatial variations of riverine carbon in the Shaliu River.

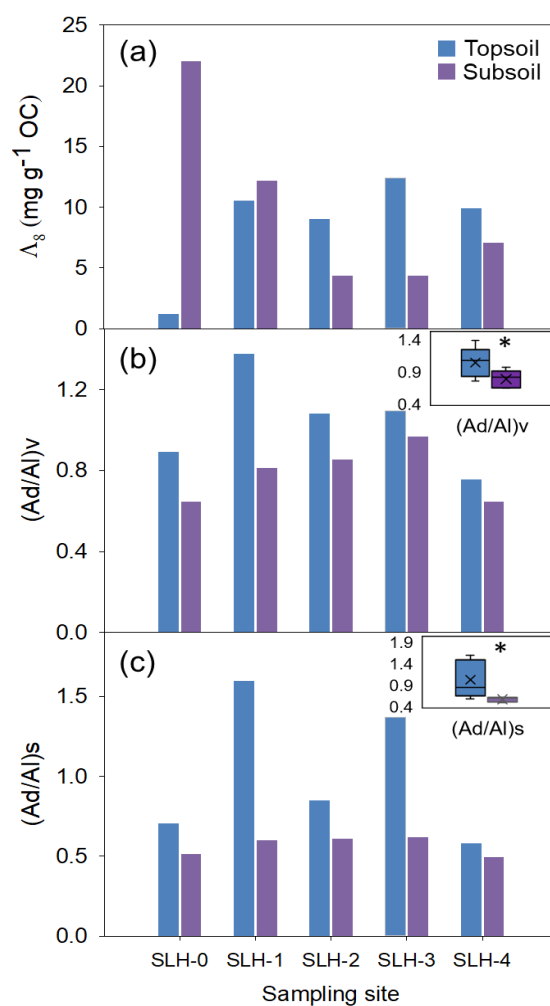


215 **Figure 3.** Variations of dissolved organic carbon (DOC) in Shaliu River water (a), absolute concentration of lignin phenols
 (Σ_8) in riverine dissolved organic matter (DOM; b) and particulate organic matter (POM; c) during the pre-monsoon and
 monsoon seasons in 2015, the acid-to-aldehyde (Ad/Al) ratios of syringyl (S) and vanillyl (V) phenols in the riverine DOM,
 POM, soil solutions and leachates (d). The abscissa in panel (a) means the distance of sampling sites from SLH-0. The red
 220 line in panel (a) correspond to the linear regression of data ($p < 0.05$), and the grey shaded region in panel (a) show 95%
 confidence intervals. The inserted box in (d) is the comparison of $(Ad/Al)_v$ and $(Ad/Al)_s$ ratios of dissolved lignin phenols
 between pre-monsoon and monsoon seasons, respectively, with asterisks indicating significant differences (independent
 sample t tests, $n = 5$, $p < 0.05$). The solid bar and cross in the inserted box mark the median and mean of each data set,
 respectively. The upper and lower ends of box denote the 0.25 and 0.75 percentiles, respectively. NA, not analyzed.

Both $(Ad/Al)_v$ and $(Ad/Al)_s$ ratios of dissolved lignin phenols, fluctuating along the Shaliu River, were consistently lower
 225 in the pre-monsoon than monsoon season (Figure 3d), consistent with the Arctic rivers (Amon et al., 2012) but different from
 the invariant or opposite patterns between seasons in tropical rivers including Congo and Oubangui (Spencer et al., 2010b;
 Bouillon et al., 2012). Higher acid-to-aldehyde ratio of lignin phenols is commonly attributed to increased photo- or
 microbial oxidation of lignin. However, photo- and microbial oxidation may be partially constrained by the short residence



time (indicated by high discharge in monsoon season) and low temperature in this alpine headstream (average water
230 temperature of 10.8°C in the monsoon season; Table S2). After examining lignin phenols in the soils of the Shaliu basin, we
found spatially variable concentrations of lignin phenols (Figure 4a) but consistently higher (Ad/Al)_v and (Ad/Al)_s ratios in
the top- than subsoil at all sampling sites ($p < 0.05$; Figures 4b-c). We hence postulate that topsoil makes a relatively larger
contribution to riverine DOM in the monsoon season likely through increased surface runoff, resulting in higher acid-to-
aldehyde ratios of dissolved lignin in the stream compared to the pre-monsoon season.



235

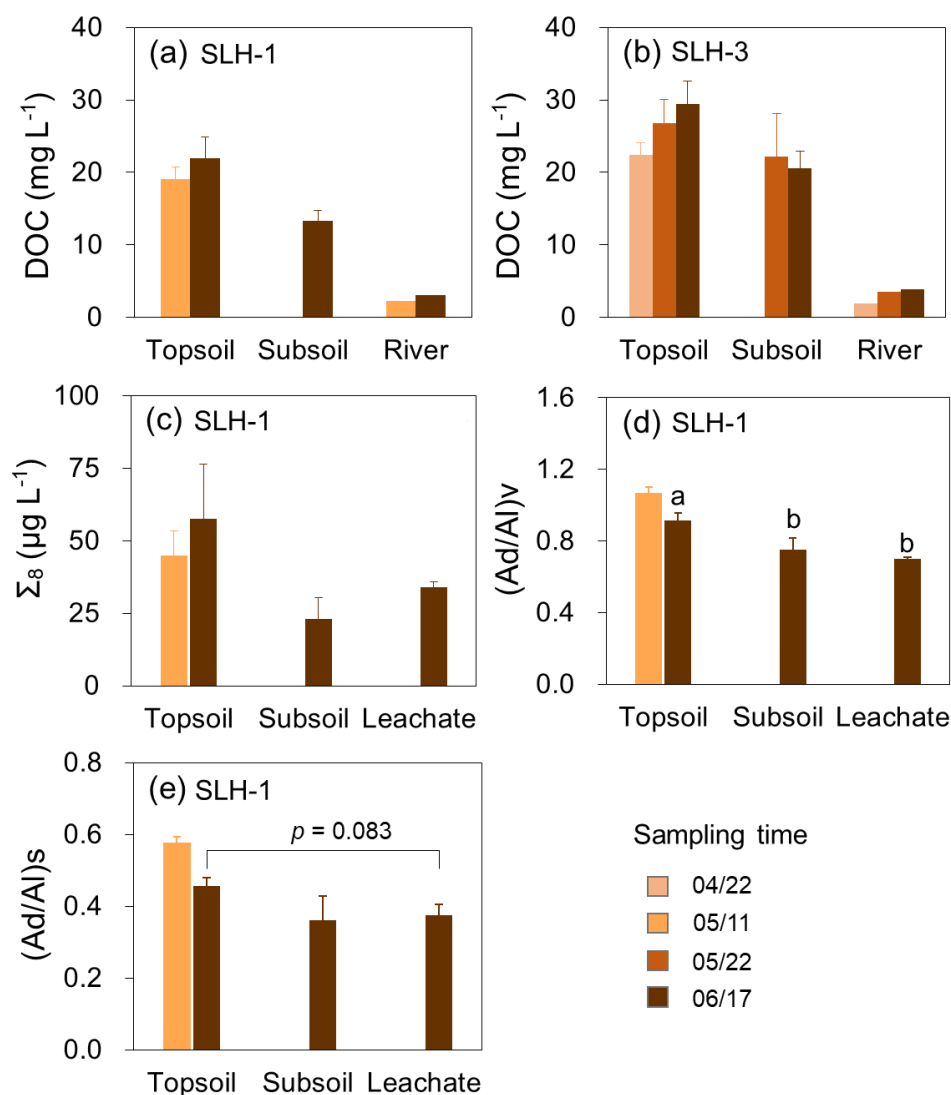
240

Figure 4. Organic carbon (OC)-normalized concentration of lignin phenols (Λ_8 , a), the acid-to-aldehyde (Ad/Al) ratios of vanillyl (V, b) and syringyl (S, c) phenols in the soil of Shaliu River basin. The solid bar and cross in the inserted boxes in panels (b) and (c) mark the median and mean of each dataset, respectively. The upper and lower ends of boxes denote the 0.25 and 0.75 percentiles, respectively. Asterisks indicate significant differences between topsoil (0–10 cm) and subsoil (40–60 cm; paired-sample t tests, $n = 5$, $p < 0.05$). The legends in panel (a) also apply to other panels.



3.3 Riverine carbon variations influenced by local hydrological events

The unique spatial-temporal variations of riverine carbon mentioned above are likely related to the high sensitivity of the Shaliu River to local hydrological processes (Biggs et al., 2017), including sporadic occurrence of local precipitation in the monsoon season (Wu et al., 2019) and thawing of seasonal permafrost in pre-monsoon (spring) season. To reveal soil-river carbon transfer inducing riverine carbon variations in the Shaliu River, we focused on two important hydrological events. First, we anticipated that the downstream increase of riverine carbon in the pre-monsoon season (April-May) was related to spring thawing releasing DOC previously frozen in the soil. We monitored DOC and lignin phenol concentrations in topsoil solutions along with the progress of thawing (when soil temperature reached $> 0^{\circ}\text{C}$). Soil DOC and lignin phenols increased from 19.1 to 22.0 mg L^{-1} and from 44.9 to 57.6 $\mu\text{g L}^{-1}$ on May 11 to June 17 at SLH-1 station, respectively (Figures 5a-c). Similarly, soil DOC increased from 22.4 to 29.4 mg L^{-1} on April 22 to June 17 at SLH-3 station (Figure 5b). Subsoil-derived DOM was gradually released with thawing, indicated by the increase of DOC (or lignin phenol) concentration from not detectable (frozen) on May 11 to 13.3 mg L^{-1} (lignin phenols = 23.1 $\mu\text{g L}^{-1}$) and 22.1 mg L^{-1} on May 22 and June 17 at SLH-1 and SLH-3 stations, respectively (Figures 5a-c). Furthermore, lignin Ad/Al ratios were lower in the leachates of thawed soils than in the topsoil solution ($p < 0.05$) but similar to the subsoil solution at SLH-1 station (Figures 5d-e), indicating significant contribution of deep soil DOM to the leachate. Concurrently, riverine DOC increased from 2.3 to 3.1 mg L^{-1} on May 11 to June 17 and from 1.9 to 3.9 mg L^{-1} on April 22 to June 17 at SLH-1 and SLH-3 stations (Figures 5a-b). This synchronous increase of DOC in river water and soil solution, at least in part, explains the downstream increase of DOC along the Shaliu River in the pre-monsoon season. With a slightly higher elevation in the upstream Shaliu basin, soil temperature is slightly lower in the upstream than downstream in spring ($-1.2\sim 0^{\circ}\text{C}$ at SLH-1 versus $0\sim 2.9^{\circ}\text{C}$ at SLH-3 on March 26 to April 20; Figure 1b), leading to earlier and stronger thawing of soil in the lower basin. Hence, inputs of DOC from thawed soil increase downstream in spring, leading to the downstream increase of riverine carbon in this alpine headwater stream.



265 **Figure 5.** Variations of dissolved organic carbon (DOC) in soil solutions and river water at SLH-1 (a) and SLH-3 (b)
 station, absolute concentration of lignin phenols (Σ_8) in soil solutions and leachates in SLH-1 station (c), and the variations
 of the acid-to-aldehyde (Ad/Al) ratios of syringyl (S) and vanillyl (V) phenols in soil solutions and leachates at SLH-1
 station (d-e) during thawing period in 2018. Error bars in panels (a-e) represent standard error of mean (n = 4). Lowercase
 letters in panel (d) indicate different levels of Ad/Al ratio among the leachates, top- and subsoil solutions (one-way ANOVA,
 270 n = 4, $p < 0.05$) while p values in panel (e) indicate marginal difference of Ad/Al ratio between topsoil solutions and
 leachates.

In contrast, sporadic local precipitation events frequently occur in the monsoon season (from June to September) on the Qinghai-Tibetan Plateau. A typically local precipitation event lasting for ~1 hour at SLH-4 station was monitored to



investigate the influence of precipitation on riverine carbon dynamics. With the start of rain, riverine DOC concentration
275 increased from 2.0 mg L⁻¹ to 3.3 mg L⁻¹ within 0.5 hour due to flushing and leaching of terrestrially derived organic matter,
and then decreased to 2.1 mg L⁻¹ at the end of precipitation event due to dilution by rainwater (Table 1). This rapid response
of riverine DOC indicates the high sensitivity of riverine carbon to short-term precipitation. According to historical
precipitation records (Zhang et al., 2013; Wu et al., 2016), more than 90% of the annual precipitation occurs in monsoon
season from June to September, mainly in the form of short-lasting and weak precipitation events (intensity < 5 mm; Wu et
280 al., 2016), thus frequently influencing local soil-stream carbon transfer processes. Along the Shaliu River, DOC
concentrations in the monsoon season showed no regular downstream variations, likely related to variable local precipitation
events frequently occurring in the Shaliu River basin in the summer (Yao et al., 2013; Wu et al., 2016).

Table 1. River water properties at the SLH-4 station of Shaliu River during a precipitation event in August 2015.

Sample	T (°C)	pH	Cond. (µs cm ⁻¹)	DO	(mg L ⁻¹)					
					TSS	DIC	DOC	PIC	POC	
SLH-4	11.4	8.2	386	5.9	5.8	37.76	2.04	0.03	0.36	
SLH-4	11.1	8.3	381	5.6	6.2	37.43	3.26	0.04	0.44	
SLH-4	11.0	8.3	384	5.5	7.0	37.24	3.21	0.04	0.42	
SLH-4	11.5	8.3	384	5.2	7.4	37.96	2.06	0.06	0.46	
Mean	11.3	8.3	384	5.6	6.6	37.60	2.64	0.04	0.42	

285 T, water temperature; Cond., conductivity; DO, dissolved oxygen; TSS, total suspended solid; DIC, dissolved
inorganic carbon; DOC, dissolved organic carbon; PIC, particulate inorganic carbon; POC, particulate organic
carbon.

4. Conclusions

In conclusion, combining annual flux monitoring and dense spatial sampling along the Shaliu River in two contrasting
290 seasons, we provide a benchmark assessment of riverine carbon dynamics in a typical alpine headwater stream on Qinghai-
Tibetan Plateau. We show that dissolved carbon (especially DIC) constitutes the majority (> 87%) of riverine carbon in this
alpine headstream, dominated by carbon fluxes in the monsoonal summer. In addition, riverine carbon in the Shaliu River
increased downstream in the pre-monsoon season due to increasing contribution of organic matter derived from thawed
seasonal permafrost while organic matter inputs induced by sporadic precipitation during the monsoon season led to
295 fluctuating levels of riverine carbon in the summer. These results indicate a high sensitivity of riverine carbon in the alpine
headwater stream to local hydrological events. Given projected climate warming on the Qinghai-Tibetan Plateau (Chen et al.,
2013), thawing of permafrost and alterations of precipitation regimes may significantly influence the alpine headwater



carbon dynamics, with cascading effects on the biogeochemical cycles of the watersheds. On the other hand, the alpine
headwater streams may be utilized as sentinels for climate-induced changes in the hydrological pathways and/or
300 biogeochemistry of the small basin. Both aspects deserve further research attention in the future.

Data availability. All data are available within this paper and in the Supplement.

Supplement. The supplement related to this article is available online.

305

Author contribution. X.F. designed the study. X.W. performed geochemical and lignin phenol analyses and analyzed related
data. X.W. and T.L. contributed equally to this work. All authors contributed to the field sampling.

Competing interests. The authors declare that they have no conflict of interest.

310 **Acknowledgements**

This study was funded by the Chinese National Key Development Program for Basic Research (2019YFA0607303) and the
National Natural Science Foundation of China (42025303; 41973075; 31988102). The authors declare no competing
financial interests.

References

- 315 Amon, R. M. W., Rinehart, A. J., Duan, S., Louchouart, P., Prokushkin, A., Guggenberger, G., Bauch, D., Stedmon, C.,
Raymond, P. A., Holmes, R. M., McClelland, J. W., Peterson, B. J., Walker, S. A., and Zhulidov, A. V.: Dissolved organic
matter sources in large Arctic rivers, *Geochimica Et Cosmochimica Acta*, 94, 217-237, 10.1016/j.gca.2012.07.015, 2012.
- Argerich, A., Haggerty, R., Johnson, S. L., Wondzell, S. M., Dosch, N., Corson-Rikert, H., Ashkenas, L. R., Pennington, R.,
and Thomas, C. K.: Comprehensive multiyear carbon budget of a temperate headwater stream, *J. Geophys. Res.-*
320 *Biogeosci.*, 121, 1306-1315, 10.1002/2015jg003050, 2016.
- Bao, H. Y., Niggemann, J., Huang, D. K., Dittmar, T., and Kao, S. J.: Different responses of dissolved black carbon and
dissolved lignin to seasonal hydrological changes and an extreme rain event, *J. Geophys. Res.-Biogeosci.*, 124, 479-493,
10.1029/2018jg004822, 2019.
- Battin, T. J., Kaplan, L. A., Findlay, S., Hopkinson, C. S., Marti, E., Packman, A. I., Newbold, J. D., and Sabater, F.: Erratum:
325 Biophysical controls on organic carbon fluxes in fluvial networks, *Nature Geoscience*, 2, 595-595, 10.1038/ngeo602,
2009.
- Benda, L., Hassan, M. A., Church, M., and May, C. L.: Geomorphology of steepland headwaters: The transition from



- hillslopes to channels, *Journal of the American Water Resources Association*, 41, 835-851, 2005.
- Biggs, J., von Fumetti, S., and Kelly-Quinn, M.: The importance of small waterbodies for biodiversity and ecosystem
330 services: implications for policy makers, *Hydrobiologia*, 793, 3-39, 10.1007/s10750-016-3007-0, 2017.
- Bouillon, S., Yambele, A., Spencer, R. G. M., Gillikin, D. P., Hernes, P. J., Six, J., Merckx, R., and Borges, A. V.: Organic
matter sources, fluxes and greenhouse gas exchange in the Oubangui River (Congo River basin), *Biogeosciences*, 9,
2045-2062, 10.5194/bg-9-2045-2012, 2012.
- Bröder, L., Davydova, A., Davydov, S., Zimov, N., Haghypour, N., Eglinton, T. I., and Vonk, J. E.: Particulate organic matter
335 dynamics in a permafrost headwater stream and the Kolyma River mainstem, *J. Geophys. Res.-Biogeosci.*, 125,
10.1029/2019jg005511, 2020.
- Cai, W.-J., Guo, X., Chen, C.-T. A., Dai, M., Zhang, L., Zhai, W., Lohrenz, S. E., Yin, K., Harrison, P. J., and Wang, Y.: A
comparative overview of weathering intensity and HCO_3^- flux in the world's major rivers with emphasis on the
Changjiang, Huanghe, Zhujiang (Pearl) and Mississippi Rivers, *Continental Shelf Research*, 28, 1538-1549,
340 10.1016/j.csr.2007.10.014, 2008.
- Caillon, F., and Schelker, J.: Dynamic transfer of soil bacteria and dissolved organic carbon into small streams during
hydrological events, *Aquatic Sciences*, 82, 10.1007/s00027-020-0714-4, 2020.
- Chang, J., Ye, R., and Wang, G.: Review: Progress in permafrost hydrogeology in China, *Hydrogeology Journal*, 26, 1387-
1399, 10.1007/s10040-018-1802-6, 2018.
- 345 Chen, H., Zhu, Q., Peng, C., Wu, N., Wang, Y., Fang, X., Gao, Y., Zhu, D., Yang, G., Tian, J., Kang, X., Piao, S., Ouyang, H.,
Xiang, W., Luo, Z., Jiang, H., Song, X., Zhang, Y., Yu, G., Zhao, X., Gong, P., Yao, T., and Wu, J.: The impacts of
climate change and human activities on biogeochemical cycles on the Qinghai-Tibetan Plateau, *Global change biology*,
19, 2940-2955, 10.1111/gcb.12277, 2013.
- Cheng, S., Cao, S., Cao, G., Han, J., Han, G., and Wu, F.: Comparisons of supervised classification methods for land cover
350 based on high spatial resolution remote sensing images in Shaliu River basin of Qinghai Lake, *Bulletin of Soil and Water
Conservation*, 38, 261-268, 2018.
- Chiasson-Poirier, G., Franssen, J., Lafreniere, M. J., Fortier, D., and Lamoureux, S. F.: Seasonal evolution of active layer
thaw depth and hillslope-stream connectivity in a permafrost watershed, *Water Resources Research*, 56,
10.1029/2019wr025828, 2020.
- 355 Dai, G., Zhu, E., Liu, Z., Wang, Y., Zhu, S., Wang, S., Ma, T., Jia, J., Wang, X., Hou, S., Fu, P., Peterse, F., and Feng, X.:
Compositional characteristics of fluvial particulate organic matter exported from the world's largest alpine wetland, *J.
Geophys. Res.-Biogeosci.*, 124, 2709-2727, 10.1029/2019jg005231, 2019.
- Dornblaser, M. M., and Striegl, R. G.: Switching predominance of organic versus inorganic carbon exports from an
intermediate-size subarctic watershed, *Geophysical Research Letters*, 42, 386-394, 10.1002/2014gl062349, 2015.
- 360 Downing, J. A., Cole, J. J., Duarte, C. M., Middelburg, J. J., Melack, J. M., Prairie, Y. T., Kortelainen, P., Striegl, R. G.,
McDowell, W. H., and Tranvik, L. J.: Global abundance and size distribution of streams and rivers, *Inland Waters*, 2,



- 229-236, 10.5268/iw-2.4.502, 2012.
- Flury, S., and Ulseth, A. J.: Exploring the sources of unexpected high methane concentrations and fluxes from alpine headwater streams, *Geophysical Research Letters*, 46, 6614-6625, 10.1029/2019gl082428, 2019.
- 365 French, D. W., Schindler, D. E., Brennan, S. R., and Whited, D.: Headwater catchments govern biogeochemistry in America's largest free-flowing river network, *Journal of Geophysical Research: Biogeosciences*, 10.1029/2020jg005851, 2020.
- Gao, T., Kang, S., Chen, R., Zhang, T., Zhang, T., Han, C., Tripathee, L., Sillanpaa, M., and Zhang, Y.: Riverine dissolved organic carbon and its optical properties in a permafrost region of the Upper Heihe River basin in the Northern Tibetan Plateau, *Science of the Total Environment*, 686, 370-381, 10.1016/j.scitotenv.2019.05.478, 2019.
- 370 Giesler, R., Lyon, S. W., Morth, C. M., Karlsson, J., Karlsson, E. M., Jantze, E. J., Destouni, G., and Humborg, C.: Catchment-scale dissolved carbon concentrations and export estimates across six subarctic streams in northern Sweden, *Biogeosciences*, 11, 525-537, 10.5194/bg-11-525-2014, 2014.
- Gomi, T., Sidle, R. C., and Richardson, J. S.: Understanding processes and downstream linkages of headwater systems, *Bioscience*, 52, 905-916, 10.1641/0006-3568(2002)052[0905:Upadlo]2.0.Co;2, 2002.
- 375 Guo, L., Cai, Y., Belzile, C., and Macdonald, R. W.: Sources and export fluxes of inorganic and organic carbon and nutrient species from the seasonally ice-covered Yukon River, *Biogeochemistry*, 107, 187-206, 10.1007/s10533-010-9545-z, 2012.
- Harrison, J. A., Seitzinger, S. P., Bouwman, A. F., Caraco, N. F., Beusen, A. H. W., and Vorosmarty, C. J.: Dissolved inorganic phosphorus export to the coastal zone: Results from a spatially explicit, global model, *Global Biogeochemical Cycles*, 19, 10.1029/2004gb002357, 2005.
- 380 Hassan, M. A., Church, M., Lisle, T. E., Brardinoni, F., Benda, L., and Grant, G. E.: Sediment transport and channel morphology of small, forested streams, *Journal of the American Water Resources Association*, 41, 853-876, 10.1111/j.1752-1688.2005.tb03774.x, 2005.
- Hedges, J. I., and Ertel, J. R.: Characterization of lignin by gas capillary chromatography of cupric oxidation-products, , *Analytical Chemistry*, 54, 174-178, 10.1021/ac00239a007, 1982.
- 385 Hernes, P. J., Robinson, A. C., and Aufdenkampe, A. K.: Fractionation of lignin during leaching and sorption and implications for organic matter "freshness", *Geophysical Research Letters*, 34, 10.1029/2007gl031017, 2007.
- Huang, T.-H., Fu, Y.-H., Pan, P.-Y., and Chen, C.-T. A.: Fluvial carbon fluxes in tropical rivers, *Curr. Opin. Environ. Sustain.*, 4, 162-169, 10.1016/j.cosust.2012.02.004, 2012.
- 390 Immerzeel, W. W., van Beek, L. P. H., and Bierkens, M. F. P.: Climate Change Will Affect the Asian Water Towers, *Science*, 328, 1382-1385, 10.1126/science.1183188, 2010.
- Jaffé, R., Yamashita, Y., Maie, N., Cooper, W. T., Dittmar, T., Dodds, W. K., Jones, J. B., Myoshi, T., Ortiz-Zayas, J. R., Podgorski, D. C., and Watanabe, A.: Dissolved organic matter in headwater streams: Compositional variability across climatic regions of North America, *Geochimica Et Cosmochimica Acta*, 94, 95-108, 10.1016/j.gca.2012.06.031, 2012.



- 395 Johnson, M. S., Lehmann, J., Couto, E. G., Novaes Filho, J. P., and Riha, S. J.: DOC and DIC in flowpaths of Amazonian headwater catchments with hydrologically contrasting soils, *Biogeochemistry*, 81, 45-57, 10.1007/s10533-006-9029-3, 2006.
- Lambert, T., Teodoru, C. R., Nyoni, F. C., Bouillon, S., Darchambeau, F., Massicotte, P., and Borges, A. V.: Along-stream transport and transformation of dissolved organic matter in a large tropical river, *Biogeosciences*, 13, 2727-2741, 10.5194/bg-13-2727-2016, 2016.
- 400 Lambert, T., Teodoru, C. R., Nyoni, F. C., Bouillon, S., Darchambeau, F., Massicotte, P., and Borges, A. V.: Along-stream transport and transformation of dissolved organic matter in a large tropical river, *Biogeosciences*, 13, 2727-2741, 10.5194/bg-13-2727-2016, 2016.
- Larouche, J. R., Abbott, B. W., Bowden, W. B., and Jones, J. B.: The role of watershed characteristics, permafrost thaw, and wildfire on dissolved organic carbon biodegradability and water chemistry in Arctic headwater streams, *Biogeosciences*, 12, 4221-4233, 10.5194/bg-12-4221-2015, 2015.
- Li, C., Li, X., Yang, T., and Li, Y.: Structure and species diversity of meadow community along the Shaliu River in the Qinghai Lake basin, *Arid Zone Research*, 30, 1028-1035, 2013.
- 405 Li, C., Li, X., Yang, T., and Li, Y.: Structure and species diversity of meadow community along the Shaliu River in the Qinghai Lake basin, *Arid Zone Research*, 30, 1028-1035, 2013.
- Liu, T., Wang, L., Feng, X., Zhang, J., Ma, T., Wang, X., and Liu, Z.: Comparing soil carbon loss through respiration and leaching under extreme precipitation events in arid and semiarid grasslands, *Biogeosciences*, 15, 1627-1641, 10.5194/bg-15-1627-2018, 2018.
- Louchouart, P., Amon, R. M. W., Duan, S., Pondell, C., Seward, S. M., and White, N.: Analysis of lignin-derived phenols in standard reference materials and ocean dissolved organic matter by gas chromatography/tandem mass spectrometry, *Marine Chemistry*, 118, 85-97, 10.1016/j.marchem.2009.11.003, 2010.
- Mann, P. J., Eglinton, T. I., McIntyre, C. P., Zimov, N., Davydova, A., Vonk, J. E., Holmes, R. M., and Spencer, R. G. M.: Utilization of ancient permafrost carbon in headwaters of Arctic fluvial networks, *Nature Communications*, 6, 10.1038/ncomms8856, 2015.
- 415 Mann, P. J., Spencer, R. G. M., Hernes, P. J., Six, J., Aiken, G. R., Tank, S. E., McClelland, J. W., Butler, K. D., Dyda, R. Y., and Holmes, R. M.: Pan-Arctic trends in terrestrial dissolved organic matter from optical measurements, *Front. Earth Sci.*, 4, 10.3389/feart.2016.00025, 2016.
- McMahon, T. A., and Finlayson, B. L.: Droughts and anti-droughts: the low flow hydrology of Australian rivers, *Freshwater Biology*, 48, 1147-1160, 10.1046/j.1365-2427.2003.01098.x, 2003.
- 420 Meyer, J. L., and Wallace, J. B.: *Lost linkages and lotic ecology: rediscovering small streams*, Ecology: Achievement and Challenge, edited by: Press, M. C., Huntly, N. J., and Levin, S., 295-317 pp., 2001.
- Opsahl, S., and Benner, R.: Early diagenesis of vascular plant-tissues-lignin and cutin decomposition and biogeochemical implications, *Geochimica Et Cosmochimica Acta*, 59, 4889-4904, 10.1016/0016-7037(95)00348-7, 1995.
- Öquist, M. G., Bishop, K., Grelle, A., Klemedtsson, L., Kohler, S. J., Laudon, H., Lindroth, A., Lofvenius, M. O., Wallin, M. B., and Nilsson, M. B.: The full annual carbon balance of boreal forests is highly sensitive to precipitation, *Environmental Science & Technology Letters*, 1, 315-319, 10.1021/ez500169j, 2014.
- 425 Pereira, R., Bovolo, C. I., Spencer, R. G. M., Hernes, P. J., Tipping, E., Vieth-Hillebrand, A., Pedentchouk, N., Chappell, N. A., Parkin, G., and Wagner, T.: Mobilization of optically invisible dissolved organic matter in response to rainstorm



- events in a tropical forest headwater river, *Geophysical Research Letters*, 41, 1202-1208, 10.1002/2013gl058658, 2014.
- 430 Prokushkin, A. S., Pokrovsky, O. S., Shirokova, L. S., Korets, M. A., Viers, J., Prokushkin, S. G., Amon, R. M. W., Guggenberger, G., and McDowell, W. H.: Sources and the flux pattern of dissolved carbon in rivers of the Yenisey basin draining the Central Siberian Plateau, *Environmental Research Letters*, 6, 14, 10.1088/1748-9326/6/4/045212, 2011.
- Qiu, J.: The third pole, *Nature*, 454, 393-396, 10.1038/454393a, 2008.
- 435 Qu, B., Sillanpaa, M., Li, C., Kang, S., Stubbins, A., Yan, F., Aho, K. S., Zhou, F., and Raymond, P. A.: Aged dissolved organic carbon exported from rivers of the Tibetan Plateau, *Plos One*, 12, 10.1371/journal.pone.0178166, 2017.
- Qualls, R. G., Haines, B. L., Swank, W. T., and Tyler, S. W.: Retention of soluble organic nutrients by a forested ecosystem, *Biogeochemistry*, 61, 135-171, 10.1023/a:1020239112586, 2002.
- Ran, L., Lu, X. X., Sun, H., Han, J., Li, R., and Zhang, J.: Spatial and seasonal variability of organic carbon transport in the Yellow River, China, *Journal of Hydrology*, 498, 76-88, 10.1016/j.jhydrol.2013.06.018, 2013.
- 440 Raymond, P. A., McClelland, J. W., Holmes, R. M., Zhulidov, A. V., Mull, K., Peterson, B. J., Striegl, R. G., Aiken, G. R., and Gurtovaya, T. Y.: Flux and age of dissolved organic carbon exported to the Arctic Ocean: A carbon isotopic study of the five largest arctic rivers, *Global Biogeochemical Cycles*, 21, 9, 10.1029/2007gb002934, 2007.
- Richardson, J. S., Naiman, R. J., Swanson, F. J., and Hibbs, D. E.: Riparian communities associated with Pacific Northwest headwater streams: Assemblages, processes, and uniqueness, *Journal of the American Water Resources Association*, 41, 445 935-947, 10.1111/j.1752-1688.2005.tb03778.x, 2005.
- Rivenbark, B. L., and Jackson, C. R.: Average discharge, perennial flow initiation, and channel initiation - Small Southern Appalachian basins, *Journal of the American Water Resources Association*, 40, 639-646, 10.1111/j.1752-1688.2004.tb04449.x, 2004.
- Runkel, R. L., Crawford, C. G., and Cohn, T. A. (2004). Load estimator (LOADEST): A FORTRAN program for estimating 450 constituent loads in streams and rivers. In U.S. Geological Survey Techniques and Methods Book (Chap. A5, Vol. 4, p. 69). Denver, CO: US Geological Survey.<https://doi.org/10.3133/tm4A5>
- Seitzinger, S. P., Harrison, J. A., Dumont, E., Beusen, A. H. W., and Bouwman, A. F.: Sources and delivery of carbon, nitrogen, and phosphorus to the coastal zone: An overview of Global Nutrient Export from Watersheds (NEWS) models and their application, *Global Biogeochemical Cycles*, 19, 10.1029/2005gb002606, 2005.
- 455 Song, C., Wang, G., Mao, T., Chen, X., Huang, K., Sun, X., and Hu, Z.: Importance of active layer freeze-thaw cycles on the riverine dissolved carbon export on the Qinghai-Tibet Plateau permafrost region, *PeerJ*, 7, e7146, 10.7717/peerj.7146, 2019.
- Song, C., Wang, G., Haghpor, N., and Raymond, P. A.: Warming and monsoonal climate lead to large export of millennial-aged carbon from permafrost catchments of the Qinghai-Tibet Plateau, *Environmental Research Letters*, 15, 460 10.1088/1748-9326/ab83ac, 2020.
- Spencer, R. G. M., Aiken, G. R., Wickland, K. P., Striegl, R. G., and Hernes, P. J.: Seasonal and spatial variability in dissolved organic matter quantity and composition from the Yukon River basin, Alaska, *Global Biogeochemical Cycles*,



- 22, 10.1029/2008gb003231, 2008.
- Spencer, R. G. M., Aiken, G. R., Dyda, R. Y., Butler, K. D., Bergamaschi, B. A., and Hernes, P. J.: Comparison of XAD with
465 other dissolved lignin isolation techniques and a compilation of analytical improvements for the analysis of lignin in
aquatic settings, *Organic Geochemistry*, 41, 445-453, 10.1016/j.orggeochem.2010.02.004, 2010a.
- Spencer, R. G. M., Hernes, P. J., Ruf, R., Baker, A., Dyda, R. Y., Stubbins, A., and Six, J.: Temporal controls on dissolved
organic matter and lignin biogeochemistry in a pristine tropical river, Democratic Republic of Congo, *J. Geophys. Res.-
Biogeosci.*, 115, 10.1029/2009jg001180, 2010b.
- 470 Striegl, R. G., Dornblaser, M. M., Aiken, G. R., Wickland, K. P., and Raymond, P. A.: Carbon export and cycling by the
Yukon, Tanana, and Porcupine rivers, Alaska, 2001-2005, *Water Resources Research*, 43, 10.1029/2006wr005201, 2007.
- Svec, J. R., Kolka, R. K., and Stringer, J. W.: Defining perennial, intermittent, and ephemeral channels in Eastern Kentucky:
Application to forestry best management practices, *For. Ecol. Manage.*, 214, 170-182, 10.1016/j.foreco.2005.04.008,
2005.
- 475 Tank, S. E., Raymond, P. A., Striegl, R. G., McClelland, J. W., Holmes, R. M., Fiske, G. J., and Peterson, B. J.: A land-to-
ocean perspective on the magnitude, source and implication of DIC flux from major Arctic rivers to the Arctic Ocean,
Global Biogeochemical Cycles, 26, 15, 10.1029/2011gb004192, 2012.
- Tarnocai, C., Canadell, J. G., Schuur, E. A. G., Kuhry, P., Mazhitova, G., and Zimov, S.: Soil organic carbon pools in the
northern circumpolar permafrost region, *Global Biogeochemical Cycles*, 23, 11, 10.1029/2008gb003327, 2009.
- 480 Tittel, J., Buettner, O., Freier, K., Heiser, A., Sudbrack, R., and Ollesch, G.: The age of terrestrial carbon export and rainfall
intensity in a temperate river headwater system, *Biogeochemistry*, 115, 53-63, 10.1007/s10533-013-9896-3, 2013.
- Walvoord, M. A., and Striegl, R. G.: Increased groundwater to stream discharge from permafrost thawing in the Yukon River
basin: Potential impacts on lateral export of carbon and nitrogen, *Geophysical Research Letters*, 34, 6,
10.1029/2007gl030216, 2007.
- 485 Wang, Y., Spencer, R. G. M., Podgorski, D. C., Kellerman, A. M., Rashid, H., Zito, P., Xiao, W., Wei, D., Yang, Y., and Xu,
Y.: Spatiotemporal transformation of dissolved organic matter along an alpine stream flow path on the Qinghai-Tibet
Plateau: importance of source and permafrost degradation, *Biogeosciences*, 15, 6637-6648, 10.5194/bg-15-6637-2018,
2018.
- Waterloo, M. J., Oliveira, S. M., Drucker, D. P., Nobre, A. D., Cuartas, L. A., Hodnett, M. G., Langedijk, I., Jans, W. W. P.,
490 Tomasella, J., de Araujo, A. C., Pimentel, T. P., and Munera Estrada, J. C.: Export of organic carbon in run-off from an
Amazonian rainforest blackwater catchment, *Hydrological Processes*, 20, 2581-2597, 10.1002/hyp.6217, 2006.
- Wiegner, T. N., Seitzinger, S. P., Glibert, P. M., and Bronk, D. A.: Bioavailability of dissolved organic nitrogen and carbon
from nine rivers in the eastern United States, *Aquatic Microbial Ecology*, 43, 277-287, 10.3354/ame043277, 2006.
- Wu, H., Li, X.-Y., Li, J., Jiang, Z., Chen, H., Ma, Y., and Huang, Y.: Differential soil moisture pulse uptake by coexisting
495 plants in an alpine *Achnatherum splendens* grassland community, *Environmental Earth Sciences*, 75, 10.1007/s12665-
016-5694-2, 2016.



- Wu, H., Zhao, G., Li, X.-Y., Wang, Y., He, B., Jiang, Z., Zhang, S., and Sun, W.: Identifying water sources used by alpine riparian plants in a restoration zone on the Qinghai-Tibet Plateau: Evidence from stable isotopes, *Science of the Total Environment*, 697, 10.1016/j.scitotenv.2019.134092, 2019.
- 500 Yang, Y., Fang, J., Tang, Y., Ji, C., Zheng, C., He, J., and Zhu, B.: Storage, patterns and controls of soil organic carbon in the Tibetan grasslands, *Global change biology*, 14, 1592-1599, 10.1111/j.1365-2486.2008.01591.x, 2008.
- Yao, T. D., Masson-Delmotte, V., Gao, J., Yu, W. S., Yang, X. X., Risi, C., Sturm, C., Werner, M., Zhao, H. B., He, Y., Ren, W., Tian, L. D., Shi, C. M., and Hou, S. G.: A review of climatic controls on delta O-18 in precipitation over the Tibetan Plateau: observations and simulations, *Rev. Geophys.*, 51, 24, 10.1002/rog.20023, 2013.
- 505 Zhang, F., Jin, Z., Li, F., Yu, J., and Xiao, J.: Controls on seasonal variations of silicate weathering and CO₂ consumption in, two river catchments on the NE Tibetan Plateau, *Journal of Asian Earth Sciences*, 62, 547-560, 10.1016/j.jseaes.2012.11.004, 2013.
- Zhang, S.-Y., and Li, X.-Y.: Soil moisture and temperature dynamics in typical alpine ecosystems: a continuous multi-depth measurements-based analysis from the Qinghai-Tibet Plateau, China, *Hydrol. Res.*, 49, 194-209, 10.2166/nh.2017.215,
- 510 2018.
- Zolkos, S., Tank, S. E., and Kokelj, S. V.: Mineral weathering and the permafrost carbon-climate feedback, *Geophysical Research Letters*, 45, 9623-9632, 10.1029/2018gl078748, 2018.
- Zou, D., Zhao, L., Sheng, Y., Chen, J., Hu, G., Wu, T., Wu, J., Xie, C., Wu, X., Pang, Q., Wang, W., Du, E., Li, W., Liu, G., Li, J., Qin, Y., Qiao, Y., Wang, Z., Shi, J., and Cheng, G.: A new map of permafrost distribution on the Tibetan Plateau,
- 515 *Cryosphere*, 11, 2527-2542, 10.5194/tc-11-2527-2017, 2017.